International Research Journal of Advanced Engineering and Science
ISSN (Online): 2455-9024

# Aerodynamic Performance Analysis of Horizontal Axis Wind Turbines using Improved Blade Element Momentum Method

Verdy A Koehuan[1]
[1]Department of Mechanical Engineering, Nusa Cendana University, Kupang, NTT, Indonesia-85000

***Abstract*****—** *This study aims to analyze the aerodynamic performance of horizontal axis wind turbines through the implementation of the blade element momentum (BEM) method. The operating conditions of the rotor at high wind speeds that occur stall on the rotor so that the characteristics of 2D airfoils cannot be directly used but must be modified so that the accuracy of the prediction of wind turbine rotor performance by the BEM method can be better. The maximum power coefficient predicted TSR=6 with $C_{P,max}$=0.461 which is lower than 1.39% of the experimental results. Prediction performance of the rotor turbine through the improved BEM method showing results quite close to an experiment in which a numerical model with BEM method has been validated in this study.*

***Keywords*****—** *Blade element momentum; aerodynamic performance; airfoil characteristics; wind turbine; tip loss correction.*

## I. INTRODUCTION

Design and analysis of the aerodynamic performance of horizontal axis wind turbine is a commonly used blade element momentum (BEM) method. The advantage of this method is very easy to implement in a computer program and has fast computation time in obtaining rotor design with optimal aerodynamic characteristics. Aerodynamic characteristics such as blade geometry (rotor diameter, aerodynamic airfoil, chord, twist, and pitch) and aerodynamic forces of the turbine rotor can be easily evaluated through the use of the BEM method [1]. However, this BEM method still has a disadvantage, especially in analyzing the fluid dynamic losses in the tip and the hub is still a hot issue of research on the performance of the wind turbine rotor. Many studies have been done with this BEM improvise on methods to improve the accuracy and stability of computing in analyzing the aerodynamic performance of the turbine rotor [2][3][4]. In addition, the performance of turbine rotors can be improved through improvisation BEM theory with parameter optimization of aerodynamics and improved geometry of the blade, which was further validated through experiments [5][6][7].

BEM method is based on the Glauert theory of propeller, has undergone many modifications to improve the accuracy of calculation and computation stability [1][8]. The maximum power coefficient modern utility-scale HAWT in practice very limited improvement. This deficiency is caused by aerodynamic losses in the tip, blade inboard, and blade hub. Blade in the hub (approximately below 25% of the rotor) is designed to withstand the bending moment blade [9]. For structural integrity, relatively thick and airfoil selected in this area, which is aerodynamically unfavorable. Dumitrescu et al., 2009 showed that the hub flow separation in the region causes backflow, thus worsening the aerodynamic performance of the rotor blade [10]. A systematic diagnostic study by Sharma et al. (2010), has revealed that these constraints reduce the aerodynamic efficiency of the turbine is about 5% [11].

In general lift and drag forces are projected at a certain angle of attack at every segment along the blade following the 2D airfoil test data. Airfoil aerodynamic characteristics are the conditions will be very different 2D on 3D shape, because it is influenced by the effects of blade rotation, especially in the conditions of a large angle of attack. The blade inboard as a whole experienced the rotation following the direction of rotation of the rotor, which is a resultant force generated lift and drag producing a torque on the rotor. Viterna, et al. 1981 demonstrated a series of empirical equations to stall phenomena and the effects of blade rotation successfully predict the performance of a turbine rotor taking into account the characteristics of the airfoil [12]. Therefore, 3D airfoil characteristics should be well understood that the calculation of the forces on the turbine rotor can be predicted exactly [13].

This study aims to analyze the aerodynamic characteristics of the horizontal axis wind turbine through the improved BEM method. The improved BEM method is applied with a flowchart iterative procedure to the design parameters of the wind turbine rotor similar to the experimental results by a source of scientific articles. Turbine design parameters in the model validation is a rotor diameter of 0.944 m with the condition, $C_{P,max}$=0.468 at TSR=6 with a wind velocity 11.5 m/s (1395 rpm rotor rotation) [14].

## II. BLADE ELEMENT MOMENTUM THEORY

Blade element momentum (BEM) theory is a method that is the oldest and most commonly used in calculating the induction factor velocity of wind turbine blades. This theory is an extension of the theory of a rotating disk that was first proposed by pioneer propeller Rankine and Froude in the 19th century. The BEM theory, usually associated with Betz and Glauert's theory, but in fact, the origin of these two theories differs between the blade element momentum theory and the theory of momentum. The modern wind turbine design is done through a computer program, based on the blade element momentum (BEM) method. The basic method of BEM assumes the rotor can be analyzed as many free elements in the longitudinal direction of the blade. The velocity is induced in each element is determined by the balance of momentum in



Verdy A Koehuan, "Aerodynamic Performance Analysis of Horizontal Axis Wind Turbines using Improved Blade Element Momentum Method," *International Research Journal of Advanced Engineering and Science*, Volume 7, Issue 1, pp. 1-8, 2021.

the control volume contained a blade element. Aerodynamic forces on each element can be calculated by use of lift and drag coefficients of empirical data measuring in the wind tunnel with geometric angle of attack (AOA) rotor element relative to local velocity.

Standard Blade Element Momentum (BEM) using Prandtl blade tip loss correction that relies on simplifying assumptions vortex with optimal operating conditions and there is no expansion of the wake flow. A blade tip loss correction renewed for implementation in the formulation of the BEM theory has been developed using the lifting line method to account for the effects of expansion wake flow, roll-up, and distortion in all operating conditions. Using this model all the physical representations of the flow can be observed and hence the performance of the turbine with BEM code can be improved [15]. Amendments to the blade tip losses, originally developed for 1D (BEM), are now extended to computational models 2D Navier-Stokes Actuator Disc and 3D computational model Actuator line Navier-Stokes [16]. The results showed that there are differences between actuator disk and actuator line model, particularly at lower TSR (tip speed ratio). It is acceptable for disk actuator models are only valid in the asymmetrical flow, while at the lower TSR flow is asymmetrical. Liu S., et al. develop BEM models to improve the formulation blade tip loss calculation, empirical correction Buhl, wake vortex effect, and the effect of rotation [13]. This correction is necessary for the understanding of the turbulent flow method for the configuration of horizontal axis wind turbines (HAWT). The results of this study were compared with data NREL measured of the two models of the blade (UAE) turbine phase-VI. The results showed an upward trend with the incorporation of these corrections. BEM analysis showed that the blade design with a twist angle and the right pitch, and the target TSR appropriate, can lead to a substantial increase (over 10%) in the performance of the turbine.

Advantages BEM theory is that each element is described as an airfoil blade in two dimensions as in Fig. 1 with the velocity and angle to determine the forces on the blade element and also induction flow velocity of the wake. Fig. 2 shows the resultant aerodynamic forces on the blade element and component forces perpendicular or parallel to the rotor field. Components of these styles are known as thrust (perpendicular) and torque (parallel) to the plane of rotation, which are the dominant forces in the turbine design. In Fig. 2, the corner that connects the lift and drag with the thrust and torque are local inflow angles, φ. As shown in Fig. 1, the angle of this inflow is the sum of the local blade pitch angle, β, and the angle of attack, α. Local pitch angle depending on the geometry of blade static, elastic deflection, passive or active control systems used in blade pitch. The angle of attack is a function of the local velocity vector, which is limited by local wind speed rotor incoming (incoming wind speed increases, followed by an increase in the angle of attack), the rotor speed, blade element speed, and induction factors.

Lift and drag coefficients are defined as non-dimensional numbers as the following equation:

$$C_L = \frac{F_L}{0.5\rho V^2 c} \quad (1)$$

$$C_D = \frac{F_D}{0.5\rho V^2 c} \quad (2)$$

The relative movement of blade and direction of the lift and drag force, with the angle of attack and blade twist angle β, and the angle φ formed by the flow of the relative velocity and the chord line, as shown in Fig. 1. The relative velocity $V_{rel}$ , the angle of inflow, $\varphi = \alpha + \beta$ when,

$$V_{rel} \sin\varphi = V_\infty (1-a) \quad (3)$$

and

$$V_{rel} \cos\varphi = \omega r (1+a') \quad (4)$$

$$\tan\varphi = \frac{(1-a)V_\infty}{(1+a')\omega r} \quad (5)$$

From this it can be calculated relative velocity using the equation:

$$V_{rel}^2 = U_\infty^2 (1-a)^2 + r^2\omega^2 (1+a')^2 \quad (6)$$

Value $C_L$ and $C_D$ to $\varphi = \alpha + \beta$ be obtained from a table or chart used airfoil characteristics. Outlining the lift force and drag force on airfoils become a tangential force and the normal force can be illustrated in Fig. 2.

$$F_N = F_L \cos\varphi + F_D \sin\varphi \quad (7)$$

$$F_T = F_L \sin\varphi - F_D \cos\varphi \quad (8)$$

Furthermore, the normal force and tangential force coefficient can be written in the form of style as follows:

$$C_N = \frac{F_N}{0.5\rho {V_{rel}}^2 c} \quad (9)$$

$$C_T = \frac{F_T}{0.5\rho {V_{rel}}^2 c} \quad (10)$$

Where: $C_N = C_L \cos\varphi + C_D \sin\varphi$ and $C_T = C_L \sin\varphi - C_D \cos\varphi$

Component induction factors *a* and *a'* in (3 to 5) are a function of the forces acting on the blade and we use BEM theory to calculate it. If known nondimensional coefficient, $C_L$ and $C_D$, the number of blade *B*, and chord length *c*, then the resultant force, power, and torque respectively can be searched as the following, from the theory of BEM, thrust which is distributed around an annulus with a distance *dr* is equivalent to,

$$dT = B\frac{1}{2}\rho V_{rel}^2 (C_L \cos\varphi + C_D \sin\varphi) c\, dr \quad (11)$$

and the torque produced by the blade element in the annulus is equivalent to,

$$dQ = B\frac{1}{2}\rho V_{rel}^2 (C_L \sin\varphi - C_D \cos\varphi) c\, r\, dr \quad (12)$$

Power:

$$dP = \Omega\, dQ = \tfrac{1}{2}\rho V_{rel}^2\, \Omega r \left[C_L \sin\varphi - C_D \cos\varphi\right] B c\, dr \quad (13)$$



Verdy A Koehuan, "Aerodynamic Performance Analysis of Horizontal Axis Wind Turbines using Improved Blade Element Momentum Method," *International Research Journal of Advanced Engineering and Science*, Volume 7, Issue 1, pp. 1-8, 2021.

International Research Journal of Advanced Engineering and Science
ISSN (Online): 2455-9024

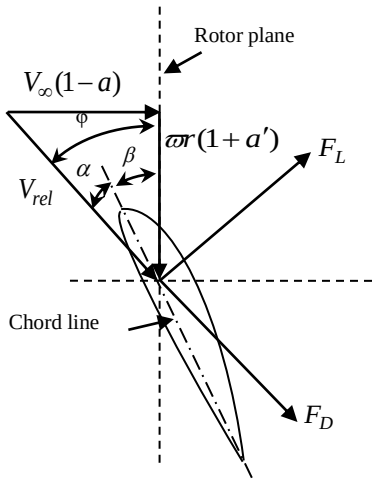


Fig. 1. Local speed and flow angle of the airfoil (blade element)

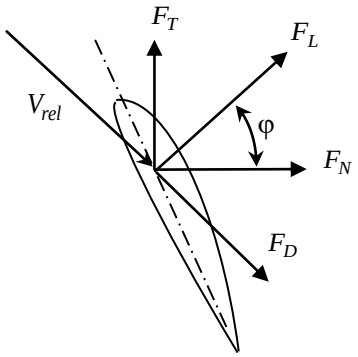


Fig. 2. The forces on the airfoil (blade element)

Thus, if on the table with a two-dimensional airfoil data input lift coefficient and drag coefficient as a function of angle of attack *α*, the equation is solved by iterating the induction velocity and the forces on each element blade. However, before we solve the equation system, we must make some corrections to the BEM theory. These corrections include model-loss tip and hub-loss to calculate the vortices shed happens.

Prandtl simplifies turbine wake flow by modeling the wake-shaped vortex screw described as a component vortex flow and the absence of a direct effect on the flow of the wake itself. This theory is expressed by a correction factor on the speed of the induction field, *F*, and can be expressed by the following equation:

$$F = \frac{2}{\pi}\cos^{-1} e^{-f} \tag{14}$$

Where:

$$f = \frac{B}{2}\frac{R-r}{r\sin\varphi} \tag{15}$$

Not much different from tip-loss, hub-loss as well as to correct the induction factor generated by a vortex flow near the hub. Hub-loss using a similar approach-loss tip. Prandtl outlining the vortex effect flow by changing (15) as follows:

$$f = \frac{B}{2}\frac{r-R_{hub}}{r\sin\varphi} \tag{16}$$

At a certain element, may be affected by local aerodynamic tip loss or damages hub, in which case the correction factor tip losses and damages hub multiplied to obtain the total loss factor.

$$F_{tot} = F_{tip}\,.\,F_{hub} \tag{17}$$

Now, to connect the induction factor in the field with the style elements in (11) and (12) we have to include part of the momentum, which indicates that the thrust and torque are extracted by each annulus is equivalent to entering a correction factor, so that:

$$dT = 4\pi r\rho U_\infty^2 (1-a)a\cos^2\varphi\, F_{tot}\, dr \tag{18}$$

and torque:

$$dQ = 4\pi r^3\rho U_\infty \Omega(1-a)a'\cos^4\varphi F_{tot}\, dr \tag{19}$$

When compared with (12) and (13),

$$dT \text{ (blade element)} = dT \text{ (momentum)}\, F_{tot} \tag{20}$$

$$dQ \text{ (blade element)} = dQ \text{ (momentum)}\, F_{tot} \tag{21}$$

By entering guesses initial value *a* and *a'*, then iterate to get the new value of *a* and *a'* so BEM equation in (20) and (21) are met, or otherwise by Moriarty (2005) with the following equation [17]:

$$C_T = \left[1+\frac{\sigma(1-a)^2\ \left(C_L\cos\varphi+C_D\sin\varphi\right)}{F\sin^2\varphi}\right] \quad a < 0{,}4 \tag{22}$$

And solidity, which is the ratio of the rotor blade to the broad sweep (swept) in total is,

$$\sigma = \frac{Bc}{2\pi r} \tag{23}$$

$$a = \left[1+\frac{4F\sin^2\varphi}{\sigma'\left(C_L\cos\varphi+C_D\sin\varphi\right)}\right]^{-1} \tag{24}$$

While tangential induction factor:

$$a' = \left[-1+\frac{4F\sin\varphi\cos\varphi}{\sigma'\left(C_L\sin\varphi-C_D\cos\varphi\right)}\right]^{-1} \tag{25}$$

Another drawback of the BEM theory is that when the induction factor is greater than 0.4, the theory is no longer valid. This happens on a turbine that operates at a high tip-speed ratio (turbine speed remained at low wind speeds), when the rotor work this is known as a wake of turbulent flow conditions ($a > 0.5$). Based on the theory of momentum, these operating conditions when some flow in the area upstream forming reversal wake flow, which is where it is no longer appropriate basic assumptions of the theory of BEM. Physically, this reversal cannot happen, what happens is the number of wakes that flow from the outside and increase turbulence. Flow behind the propeller slowed down, but the driving force (thrust) in the rotor continues to rise. As compensation for the effects of this loss, Glauert (1926) developed a correction on the rotor thrust coefficient that is based on experiments on rotor helicopters with a high induction factor. This model was initially developed as a correction to the coefficient of a rotor thrust, it has also been



Verdy A Koehuan, "Aerodynamic Performance Analysis of Horizontal Axis Wind Turbines using Improved Blade Element Momentum Method," *International Research Journal of Advanced Engineering and Science*, Volume 7, Issue 1, pp. 1-8, 2021.

used to correct the local coefficient on blade element theory. Therefore, it is important to understand the relationship between Glauert corrections with tip-loss. When the blade is near the tip height loss, the induction factor is too high; therefore, the possibility of an increase in the turbulent wake near the tip of the blade. Thus, each element of the total induced velocity should use a combination of tip-loss correction and correction Glauert. Buhl (2004) has lowered a modification to the empirical relationship Glauert which includes tip-loss correction as follows [18]:

$$C_T = \frac{8}{9} + \left(4F - \frac{40}{9}\right)a + \left(\frac{50}{9} - 4F\right)a^2 \quad a \geq 0.4 \quad (26)$$

or to calculate the induction factor,

$$a = \frac{18F - 20 - 3\left(C_T(50 - 36F) + 12F(3F - 4)\right)^{0.5}}{36F - 50} \quad (27)$$

This relationship is necessary to eliminate instability calculations while using Glauert correction to calculate thrust elements to the correction of tip-loss models. However, Dai et al, 2011 by equating (26) and (22) obtained a better relationship in calculating the value of *a*, [19], $H = \left(18F\sigma C_N \sin^2\phi + 36F^4 \sin^4\phi - 48F^3 \sin^4\phi\right)$:

$$a = \frac{0.5\left(18\sigma C_N + 36F^2 \sin^2\phi - 40F \sin^2\phi + 6H^{0.5}\right)}{9\sigma C_N - 50F \sin^2\phi + 36F^2 \sin^2\phi} \quad (28)$$

In 2005, Shen et al., proposed a correction to the tip to improve the accuracy and stability of the computational BEM theory. These models replace the function of the coefficient of thrust with a linear function of the following [2]:

$$C_T = 4\left(a_c^2 F^2 + \left(1 - 2a_c F\right)aF\right) \text{ for a} > (a_c = 1/3) \quad (29)$$

Where:

$$a = \frac{2 + Y_1 - \left(4Y_1(1 - F) + Y_1^2\right)^{0.5}}{2\left(1 + FY_1\right)} \quad (30)$$

$$Y_1 = \frac{4F \sin^2\varphi}{\sigma F_1 \left(C_L \cos\varphi + C_D \sin\varphi\right)} \quad (31)$$

$$F_1 = \frac{2}{\pi}\cos^{-1}\left[\exp\left(-g\frac{B}{2}\frac{R - r}{r\sin\varphi}\right)\right] \quad (32)$$

$$g = \exp\left[-0.125\left(B\lambda_r - 21\right)\right] + 0.1 \quad (33)$$

Lanzafame et al. 2007 through the energy equation in the field of the rotor with the notice a pressure drop that occurs and normal style, a simple formula is obtained for the radial velocity induction factor [20],

$$a' = \frac{1}{2}\left(\left(1 + \frac{4}{\lambda_r^2}a(1 - a)\right)^{0.5} - 1\right) \quad (34)$$

Airfoil characteristics used in BEM theory is the result of the analysis of 2D, so Viterna et al, 1982 propose an empirical model to modify the parameters of aerodynamic lift force and drag force in the area where the blade experienced a stall (usually at an angle of attack of more than $15^0$ [12]. Because in this region 2D airfoil characteristics are no longer valid, to model the effect of flow separation in the stall can be formulated as follows:

$$C_L = \frac{C_{D,\max}}{2}\sin 2\alpha + K_L\frac{\cos^2\alpha}{\sin\alpha} \quad (35)$$

$$C_D = C_{D,\max}\sin^2\alpha + K_D\cos\alpha \quad (36)$$

$$K_L = \left(C_{L,s} - C_{D,\max}\sin\alpha_s\cos\alpha_s\right)\frac{\sin\alpha_s}{\cos^2\alpha_s} \quad (37)$$

$$K_D = \frac{C_{D,s} - C_{D,\max}\sin^2\alpha_s}{\cos\alpha_s} \quad (38)$$

$$AR \leq 50 : C_{D,\max} = 1.11 + 0.018AR \quad (39)$$

$$AR > 50 : C_{D,\max} = 2.01 \quad (40)$$

Aspect ratio, $AR = \frac{R - r_{hub}}{c(r)}$ and $C_{D,max}$ the maximum drag coefficient which the occurrence of separation

In addition to using the model correction on the tip and hub blade, to represent the physical flow of 3D and rotational blade, Du, et al., 1998 lowered the empirical formula of the theory of flow boundary layer where the influence of the force centrifugal and decreasing pressure gradient detrimental to the cross-section of the blade as the occurrence of stall can BEM input into the model and hence the performance of the turbine with BEM models can be improved [15].

## III. METHOD

### A. Blade geometry

The blade model used in this study is the horizontal axis wind turbine adopted from the blade model developed by NORCOWE (Norwegian Centre for Offshore Wind Energy) and the Department of Energy and Process Engineering, Norwegian University of Science and Technology NTNU, Trondheim, Norway. The turbine rotor blade was developed through a series of blind tests, followed by several researchers using the airfoil S826 series issued by NREL (National Renewable Energy Laboratory). Chord length and twist angle profile along span for the blade geometry in Fig. 3. The experimental results (blind test 4) BT4 reported by Bartl and Sætran (2016) for the front turbine with a diameter of 0.944 m, $C_{P,max}$=0.468 at TSR=6 and wind speed of 11.5 m/s (1395 rpm rotor rotation) [14][21].

### B. Validation and analysis of data

The whole equation used in BEM theory outlined above, through the proposed flowchart iterative procedure in calculating induction factor, angle of attack, and aerodynamic components for each element along the blade span. To start the calculation was first performed guesses against axial and tangential induction factors (Fig. 4).

Validation of numerical models is done by calculating the error that occurred in the turbine power coefficient of the experimental results. The data used comes from the experimental results NORCOWE and NTNU. Turbine power coefficient ($C_P$) is the result of dividing the mechanical power generated rotor ($P_{out}$) and total power in the wind stream ($P_{in}$)



Verdy A Koehuan, "Aerodynamic Performance Analysis of Horizontal Axis Wind Turbines using Improved Blade Element Momentum Method," *International Research Journal of Advanced Engineering and Science*, Volume 7, Issue 1, pp. 1-8, 2021.

International Research Journal of Advanced Engineering and Science
ISSN (Online): 2455-9024

for a broad sweep of rotor given. This analysis is formulated as follows:

$$C_P = \frac{P_{out}}{P_{in}} = \frac{Q.\omega}{0.5\rho V_0^3 A} \quad (41)$$

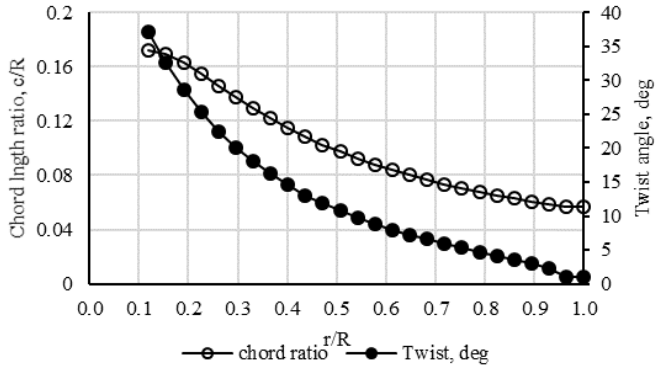


Fig. 3. Chord length and twist angle profile for blade geometry developed by NTNU using airfoil S826 series from NREL [14].

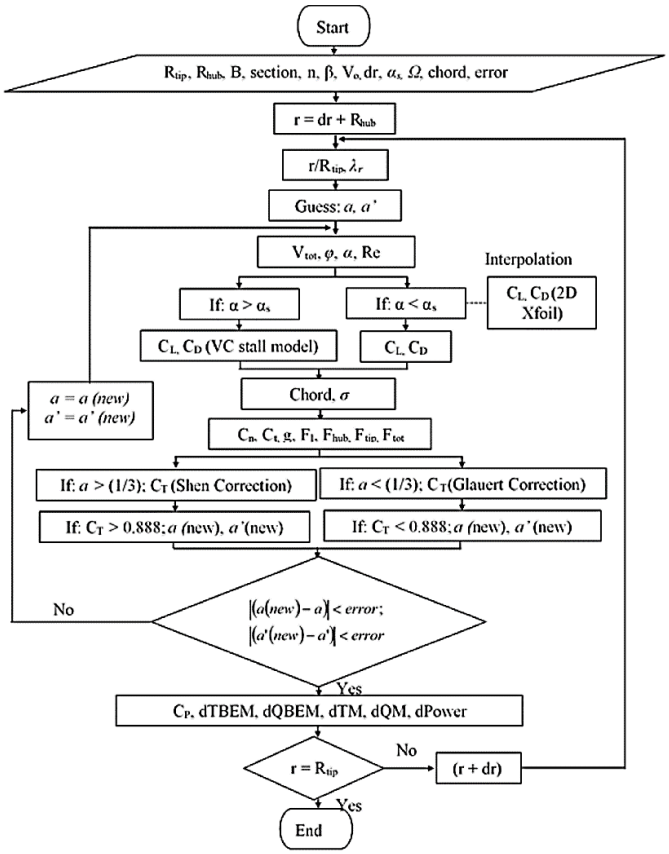


Fig. 4. Flowchart iterative procedure on blade element with improved BEM method.

The blade design in this study was adopted from the results of the blind test 4 with the same geometry, namely the diameter, twist angle, and chord length along the blade with a radius of 0.472 m. The operating conditions of the rotor were also made the same as the blind test 4 to obtain good comparison results, at TSR=6 and wind speed of 11.5 m/s (rotor rotation of 1396 rpm). The airfoil characteristic data used, namely, the S826 were obtained from 2D airfoil data (Xfoil) at the number Re=1.0E+05. Fig. 5 and Fig. 6 show the modified results of the lift coefficient and drag coefficient data from 2D airfoil data (Xfoil) and experimental data were compared.

The modified data using the BEM method through correction of Viterna et al., 1982 for the blade stalled [12]. At the angle of attack between $0^0$ to $15^0$, where the blade condition has not yet stalled so that 2D airfoil data is used by BEM in predicting turbine rotor performance. However, at an angle of attack greater than $15^0$ the blade stalled so that the 2D airfoil characteristics were no longer valid. In this case, BEM was replaced by modification of the lift and drag coefficient in that area [22]. To account for the rotor on the conditions experienced stall, then Fig. 7 shows a modified version of the airfoil lift coefficient of data using a 2D BEM. This dynamic rotor stall condition will improve prediction performance results are closer to the experimental results [23].

This modification of airfoil characteristics in stall conditions will improve the predicted results of rotor performance to be closer to the experimental results as well as improve computational stability.

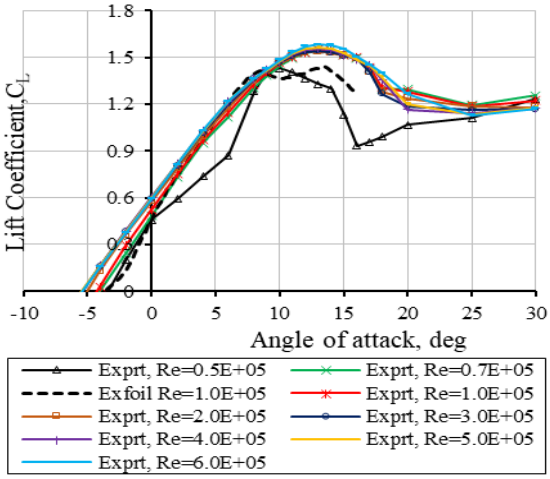


Fig. 5. Lift coefficient versus angle of attack at various Reynolds numbers plotted from data measurement [24] and Xfoil data (dashed line).

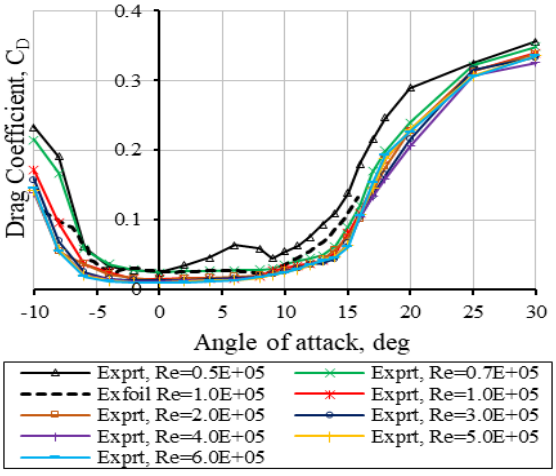


Fig. 6. Drag coefficient versus angle of attack at various Reynolds numbers plotted from data measurement [24] and Xfoil data (dashed line).



Verdy A Koehuan, "Aerodynamic Performance Analysis of Horizontal Axis Wind Turbines using Improved Blade Element Momentum Method," *International Research Journal of Advanced Engineering and Science*, Volume 7, Issue 1, pp. 1-8, 2021.

International Research Journal of Advanced Engineering and Science
ISSN (Online): 2455-9024

## IV. Results and Discussion

Fig. 7 and Fig. 8 show the relationship of lift coefficient and drag coefficient to the angle of attack respectively from the S826 2D airfoil data and the modified BEM on tip speed ratio, TSR=2 to 8. At TSR=2 to 3 the BEM prediction results show the distribution of the angle of attack along the blade is greater than $15^0$, where the blade is in a stall condition so that the Viterna correction is used for the lift and drag coefficient data [12]. While at TSR=5 to 8, the angle of attack along the blade is predicted to be less than $15^0$, so 2D airfoil data from Xfoil is used in the BEM calculation process.

The level of spread of lift and drag coefficient data on the angle of attack greatly affects the computation process using the BEM method. It can be seen that TSR=8 tends to be difficult to converge because the data distribution is quite wide and fluctuating. The spread of the fluctuating lift and drag coefficient data is due to the instability of the $a$ and $a'$ calculation results as a result of computational errors, especially in the hub area. Meanwhile, the computational error in the tip area can be reduced by applying the tip loss correction method developed by Shen et al. 2005 [16].

The axial and tangential speed induction along the span as in Fig. 9 and Fig. 10 shows the ratio of the axial speed induction ($a$) at 20%-75% of the blade length, and axial speed induction distribution is less than $a$=1/3, but in the hub area (<20%) and tip (>75%) there is an increase in the induction speed and can even reach $a$=0.5 in the tip area. This shows that in the hub and tip area there is a decrease in the conversion of kinetic energy into mechanical energy or what is known as energy losses, which is most dominant at the tip. Meanwhile, Fig. 10 shows the increase in tangential velocity ratio only occurs in the hub area, which shows that in this area there is an increase in energy losses due to the turbulent flow or vortex in that area which can be predicted by BEM (Shen correction) [2].

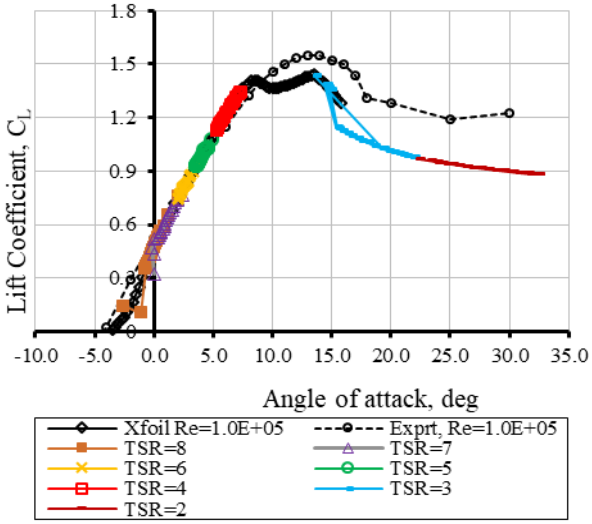


Fig. 7. Lift coefficient versus angle of attack predicted by interpolation from TSR=2 to TSR=8 combined with measured data at Re=1.0E+05 (dashed line) [24].

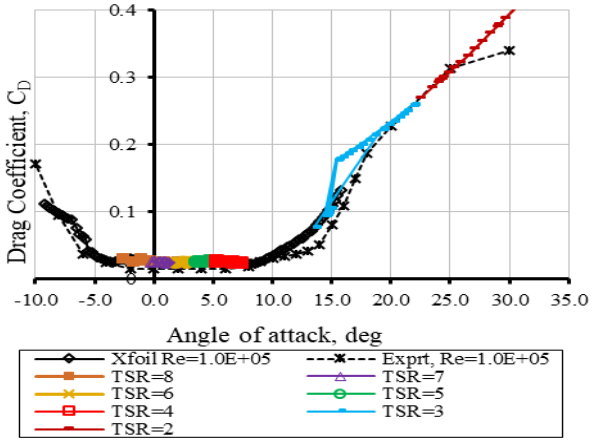


Fig. 8. Drag coefficient versus angle of attack predicted by interpolation from TSR=2 to TSR=8 combined with measured data at Re=1.0E+05 (dashed line) [24].

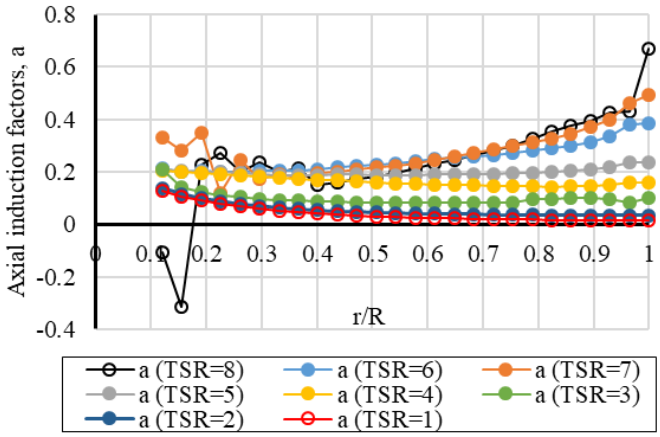


Fig. 9. Axial induction factors distribution along the span blade predicted from BEM at various tip speed ratios (TSR).

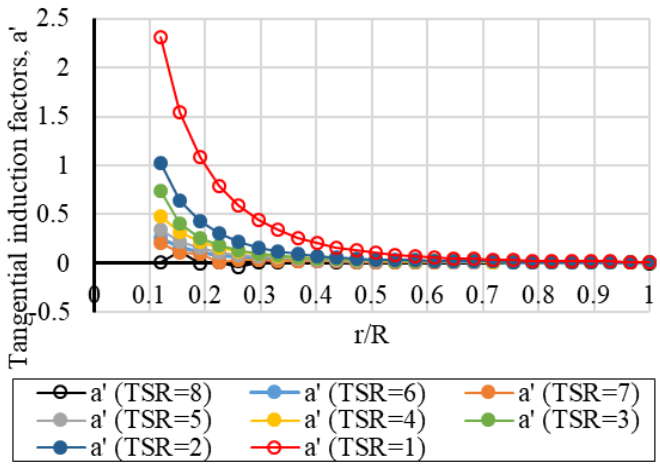


Fig. 10. Tangential induction factors distribution along the span blade predicted from BEM at various tip speed ratios (TSR).

The prediction results of wind turbine rotor performance using the BEM method are shown in the graph with the relationship between the power coefficients to the tip speed ratio (TSR) as in Fig. 11. The rotor performance through BEM predictions shows results that are quite close to the experimental results at low TSR, while the predicted results



Verdy A Koehuan, "Aerodynamic Performance Analysis of Horizontal Axis Wind Turbines using Improved Blade Element Momentum Method," *International Research Journal of Advanced Engineering and Science*, Volume 7, Issue 1, pp. 1-8, 2021.

the power coefficient with BEM at high TSR tends to be lower than the experimental results. The maximum power coefficient occurs at TSR=6 with $C_{P,max}$=0.4615 which is 1.39% lower than the experimental results of Bartl and Sætran (2016) [14]. At low TSR (TSR<4) the rotor stalls until the torque generated decreases rapidly until at TSR=1 the torque is close to zero, which means that the rotor at TSR=1 does not generate power. Also at high TSR (TSR>7) the rotor angle of attract reached a low number until at TSR=10 the generated torque drops quickly and reaches negative torque at TSR>11.5. The negative torque indicates that the rotor on the TSR is in a propeller condition. These results indicate that the numerical model with the BEM method is validated.

Fig. 11 shows the predicted results of the power coefficients to the tip speed ratio indicated that the turbine output power versus wind speed variations. Where the wind speed is lower than the turbine design wind speed ($V_0$<11.5 m/s or TSR>6) the BEM calculation lower than experimental results. This is related to the stall phenomenon that occurs in the rotor. However, at high wind speeds ($V_0$>11.5 m/s or TSR<6) the BEM results are quite close to the experimental results.

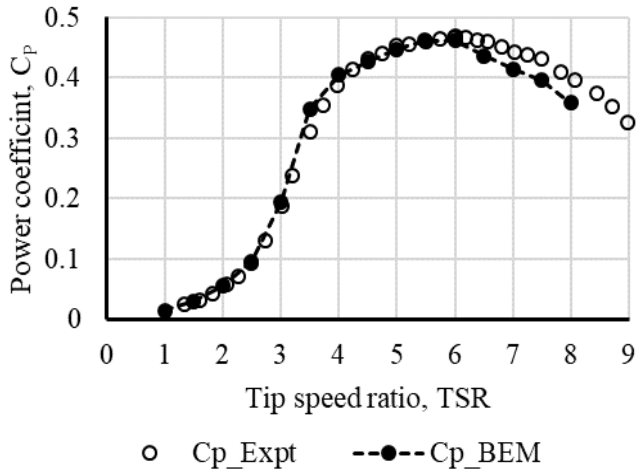


Fig. 11. Power coefficient versus tip speed ratio.

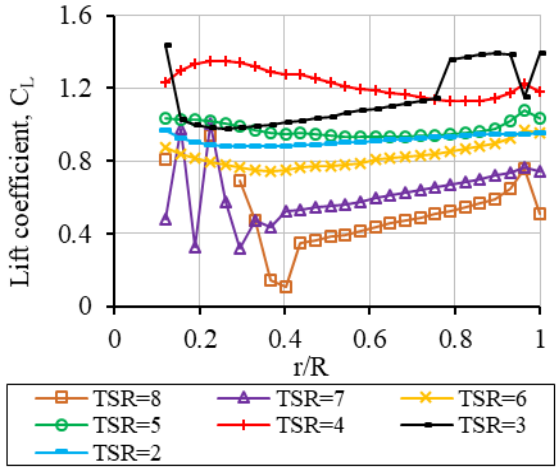


Fig. 12. Lift coefficient distribution along the span blade predicted from BEM at various tip speed ratios (TSR).

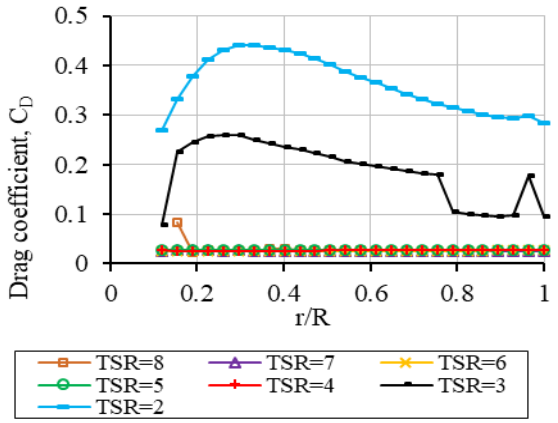


Fig. 13. Drag coefficient distribution along the span blade predicted from BEM at various tip speed ratios (TSR).

Fig. 12 and Fig. 13 show at high wind speeds or lower TSR, a stall occurs as a result of the large angle of attack for rotor operation at high wind speeds so that on the blade surface there is flow separation and an excessive negative pressure gradient which causes the higher drag force. On the other hand, at low wind speeds or high TSR, the rotor power tends to decrease as a result of the low lift generated. Therefore, the results of the prediction of turbine rotor performance are expressed as the relationship between the power coefficient and TSR as shown in Fig. 11.

## V. CONCLUSION

Prediction of propeller type horizontal axis wind turbine rotor performance through the proposed flowchart iterative procedure of BEM method shows that are quite close to the experiments. In the hub area of the blade (<0.2R) there is an increase in tangential velocity induction and conversely, in the tip area (>0.75R) an increase in axial speed induction can even reach more than 0.5 at high TSR. This shows that in the hub and tip area there is a decrease in the conversion of kinetic energy into mechanical energy or known as energy losses. The maximum power coefficient is predicted at TSR = 6 with $C_{P,max}$ = 0.4615 which is 1.39% lower than the experimental results. The operating conditions of the rotor at high wind speeds where there is a stall in the rotor so that the 2D airfoil characteristics cannot be used immediately but must be modified. So that the accuracy of the predicted results of the wind turbine rotor performance by the BEM method can be better.

## NOMENCLATURE

| | |
|---|---|
| *a* | axial velocity induction ratio |
| A | cross-sectional area ($m^2$) |
| *a'* | tangential velocity induction ratio |
| B | number of blade |
| *c* | chord length (m) |
| $C_D$ | drag force coefficient |
| $C_L$ | lift force coefficient |
| $C_N$ | normal force coefficient |
| Cp | power coefficient |
| $C_{P,max}$ | maximum power coefficient |



Verdy A Koehuan, "Aerodynamic Performance Analysis of Horizontal Axis Wind Turbines using Improved Blade Element Momentum Method," *International Research Journal of Advanced Engineering and Science*, Volume 7, Issue 1, pp. 1-8, 2021.

| | |
|---|---|
| $C_T$ | tangential force coefficient |
| $D_1$ | diameter of the first rotor (m) |
| $D_2$ | diameter of the second rotor (m) |
| F | correction factor |
| $F_D$ | drag force (N) |
| $F_L$ | lift force (N) |
| $F_N$ | normal force (N) |
| $F_T$ | tangential force (N) |
| P | power (Watt) |
| Q | torque (Nm) |
| R | radius of the rotor (m) |
| r | distance in the direction of the rotor radius (m) |
| T | *thrust* (Nm) |
| $V_\infty$ | free stream wind speed (m/s) |
| $V_{rel}$ | resultant flow velocity (m/s) |
| $\alpha$ | angle of attack |
| $\beta$ | blade angle |
| $\lambda$ | *tip speed ratio* |
| $\rho$ | density of fluid (kg/m$^3$) |
| $\sigma$ | solidity |
| $\phi$ | flow angle |
| $\omega$ | angular velocity |

## REFERENCES

[1] P. Pratumnopharat and P. S. Leung, "Validation of various windmill brake state models used by blade element momentum calculation," *Renew. energy*, vol. 36, no. 11, pp. 3222–3227, 2011.

[2] W. Z. Shen, R. Mikkelsen, J. N. Sørensen, and C. Bak, "Tip loss corrections for wind turbine computations," *Wind Energy*, vol. 8, no. 4, pp. 457–475, 2005.

[3] S. Rajakumar and D. Ravindran, "Iterative approach for optimising coefficient of power, coefficient of lift and drag of wind turbine rotor," *Renew. energy*, vol. 38, no. 1, pp. 83–93, 2012.

[4] C. J. Bai, F. B. Hsiao, M. H. Li, G. Y. Huang, and Y. J. Chen, "Design of 10 kW horizontal-axis wind turbine (HAWT) blade and aerodynamic investigation using numerical simulation," *Procedia Eng.*, vol. 67, pp. 279–287, 2013.

[5] J. R. P. Vaz, J. T. Pinho, and A. L. A. Mesquita, "An extension of BEM method applied to horizontal-axis wind turbine design," *Renew. Energy*, vol. 36, no. 6, pp. 1734–1740, 2011.

[6] M. Døssing, H. A. Madsen, and C. Bak, "Aerodynamic optimization of wind turbine rotors using a blade element momentum method with corrections for wake rotation and expansion," *Wind Energy*, vol. 15, no. 4, pp. 563–574, 2012.

[7] B. Bavanish and K. Thyagarajan, "Optimization of power coefficient on a horizontal axis wind turbine using bem theory," *Renew. Sustain. Energy Rev.*, vol. 26, pp. 169–182, 2013.

[8] R. Lanzafame and M. Messina, "Advanced brake state model and aerodynamic post-stall model for horizontal axis wind turbines," *Renew. Energy*, vol. 50, pp. 415–420, 2013, doi: 10.1016/j.renene.2012.06.062.

[9] A. Rosenberg, S. Selvaraj, and A. Sharma, "A novel dual-rotor turbine for increased wind energy capture," in *Journal of Physics: Conference Series*, 2014, vol. 524, no. 1, p. 12078.

[10] H. Dumitrescu and V. Cardos, "Inboard stall delay due to rotation," *J. Aircr.*, vol. 49, no. 1, pp. 101–107, 2012.

[11] A. Sharma, F. Taghaddosi, and A. Gupta, "Diagnosis of Aerodynamic Losses in the Root Region of a Horizontal Axis Wind Turbine," *Gen. Electr. Glob. Res. Cent. Intern. Rep.*, 2010.

[12] L. A. Viterna and R. D. Corrigan, "Fixed pitch rotor performance of large horizontal axis wind turbines," 1982.

[13] S. Liu and I. Janajreh, "Development and application of an improved blade element momentum method model on horizontal axis wind turbines," *Int. J. Energy Environ. Eng.*, vol. 3, no. 1, p. 30, 2012.

[14] J. Bartl and L. Sætran, "Blind test comparison of the performance and wake flow between two in-line wind turbines exposed to different turbulent inflow conditions," *Wind Energy Sci.*, vol. 2, no. 1, pp. 55–76, 2017.

[15] Z. Du and M. Selig, "A 3-D stall-delay model for horizontal axis wind turbine performance prediction," in *1998 ASME Wind Energy Symposium*, 1998, p. 21.

[16] W. Z. Shen, J. N. Sørensen, and R. Mikkelsen, "Tip loss correction for actuator/Navier–Stokes computations," *J. Sol. Energy Eng.*, vol. 127, no. 2, pp. 209–213, 2005.

[17] P. J. Moriarty and A. C. Hansen, "AeroDyn theory manual," National Renewable Energy Lab., Golden, CO (US), 2005.

[18] M. L. Buhl Jr, "New empirical relationship between thrust coefficient and induction factor for the turbulent windmill state," National Renewable Energy Lab.(NREL), Golden, CO (United States), 2005.

[19] J. C. Dai, Y. P. Hu, D. S. Liu, and X. Long, "Aerodynamic loads calculation and analysis for large scale wind turbine based on combining BEM modified theory with dynamic stall model," *Renew. Energy*, vol. 36, no. 3, pp. 1095–1104, 2011, doi: 10.1016/j.renene.2010.08.024.

[20] R. Lanzafame and M. Messina, "Fluid dynamics wind turbine design: Critical analysis, optimization and application of BEM theory," *Renew. energy*, vol. 32, no. 14, pp. 2291–2305, 2007.

[21] P.-Å. Krogstad and P. E. Eriksen, "'Blind test' calculations of the performance and wake development for a model wind turbine," *Renew. energy*, vol. 50, pp. 325–333, 2013.

[22] R. Lanzafame and M. Messina, "Horizontal axis wind turbine working at maximum power coefficient continuously," *Renew. Energy*, vol. 35, no. 1, pp. 301–306, 2010.

[23] G. Yu, X. Shen, X. Zhu, and Z. Du, "An insight into the separate flow and stall delay for HAWT," *Renew. Energy*, vol. 36, no. 1, pp. 69–76, 2011.

[24] J. Bartl, "Experimental testing of wind turbine wake control methods," 2018.